Synthesis and Characterization of a Model Complex for Flavodiiron NO Reductases That Stabilizes a Diiron Mononitrosyl Complex

Hai T. Dong[†,a], Yu Zong[†,a], Abigail J. Bracken[a], Michael O. Lengel[a], Jeff W. Kampf[a], Debangsu Sil[b], Carsten Krebs[b,c], Nicolai Lehnert*[,a]

[a] Department of Chemistry, The University of Michigan, Ann Arbor, Michigan 48109-1055, United States

[b] Department of Chemistry and [c] Department of Biochemistry and Molecular Biology, The Pennsylvania State University, University Park, Pennsylvania 16802, United States

[†] HTD and YZ are co-first authors

Keywords: Flavodiiron proteins, nitric oxide reductases, non-heme diiron enzymes, model complexes, second coordination sphere effects, iron-nitrosyl complexes

ABSTRACT: Flavodiiron NO reductases (FNORs) are important enzymes in microbial pathogenesis, as they equip microbes with resistance to the human immune defense agent nitric oxide (NO). DFT calculations predict that a network of second coordination sphere (SCS) hydrogen bonds is critical for the key N-N coupling step in the NO reduction reaction catalyzed by FNORs. In this study, we report the synthesis of a model complex of FNORs with pendant hydrogen bond donors. For this purpose, the ligand H[BPMP] (= 2,6-bis[[bis(2-pyridylmethyl)amino]methyl]-4-methylphenol) was modified with two amide groups in the SCS. Reaction of the precursor complex $[Fe_2(BPMP(NHCO^tBu)_2)(OAc)](OTf)_2$ (**1**) (OTf^- = triflate anion) with NO in the presence of base led to the surprising isolation of a diiron mononitrosyl complex, $[Fe_2(BPMP(NHCO^tBu)(NCO^tBu))(OAc)(NO)](OTf)$ (**2**) and a triiron decomposition product, $[Fe_3(BPMP(NHCO^tBu)_2(OAc)_2(\mu\text{-}O)_2(ONO)](OTf)$ (**3**), which were both structurally characterized. Complex **2** models the corresponding mononitrosyl adduct in FNORs. This result points towards a strategy that can be used to stabilize mononitrosyl diiron complexes, using the SCS.

Nitric oxide (NO) is an important molecule in biology, and the discovery of its relevance in many physiological and pathological events in mammals paved the way for important applications of NO in human health.[1-4] At higher, micromolar concentration, NO is an important immune defense agent that the human body uses to fight off pathogens.[5] Typically after infecting the human body, pathogens are weakened by NO and other toxic agents, generated, for example, by activated macrophages.[5,6] However, some pathogens (e.g. *Escherichia coli*, *Desulfovibrio gigas*, *Moorella thermoacetica*, *Trichomonas vaginalis*, *Klebsiella pneumoniae*, *Salmonella typhimurium*, etc.)[7-13] have evolved flavodiiron NO reductases (FNORs) to protect themselves from NO toxicity. These enzymes belong to the larger class of flavodiiron proteins (FDPs). FNORs degrade NO following the reaction:

$$2NO + 2e^- + 2H^+ \rightarrow N_2O + H_2O \qquad (1)$$

In this way, FNORs support microbial pathogenesis, leading to chronic infections that are harder to cure for our immune system.

Recent studies suggest that hydrogen bonding interactions by second coordination sphere (SCS) groups in the active sites of FNORs play a key role in catalysis, and enable direct NO reduction by these enzymes.[14-15] Specifically, mutagenesis studies using *M. thermoacetica* (*Mt*) FDP revealed a ~7-fold and ~34-fold reduction in NO reductase activity when the tyrosine and histidine residues (Y195 and H25l, respectively) in the active site are substituted for non-hydrogen bonding residues.[11] Results by Biswas et al. show that the variant Y197F of *Thermotoga maritima* (*Tm*) FDP with the hydrogen-bond donating Tyr in the active site removed has a similar affinity for NO as the wild type enzyme, leading to the formation of the critical [hs-{FeNO}^{7}]$_2$ intermediate (hs = high-spin). Here, we use the Enemark-Feltham notation {FeNO}^{n}, with n being the total number of valence electrons from the Fe(d) and NO(π*) orbitals.[16] However, at this point, the reaction stops, and the variant cannot go on to produce N_2O. These studies support the important role of hydrogen bonding interactions in the SCS in FNORs for NO reductase activity. However, structural characterization of the NO intermediates in the enzymes is challenging. Previous studies on model complexes have shown that synthetic inorganic model systems can mimic FNOR reactivity and allow for the stabilization and study of important intermediates; therefore, we set out to study these SCS interactions in well-defined diiron model complexes.[14-15, 17-21]

The ligand H[BPMP(NHCO^{t}Bu)$_2$], a variation of the ligand H[BPMP] (2,6-bis[[bis(2-pyridylmethyl)amino]methyl]-4-methylphenol), was synthesized based on a reported procedure with a modified workup as described in the Experimental Section in the SI.[22] This ligand was chosen due to the acidic proton present in the amide functional groups and the steric protection provided by the tert-butyl groups.

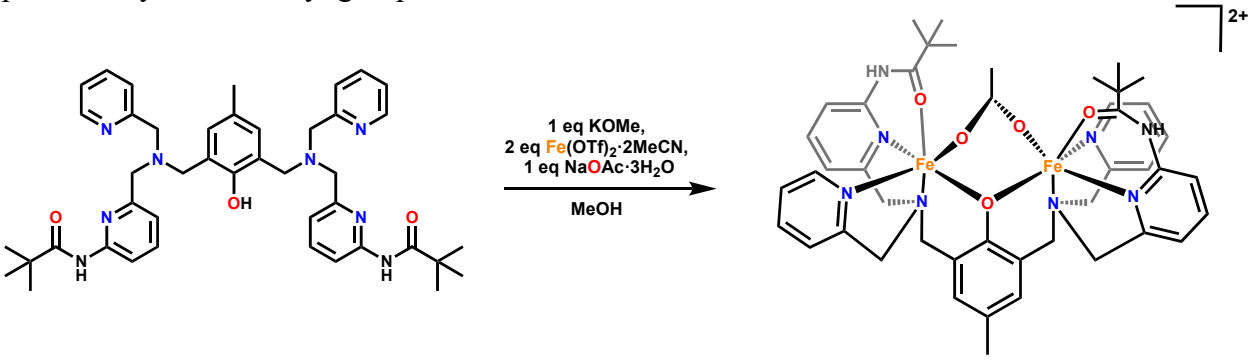

Scheme 1. Metallation of the H[BPMP(NHCO^{t}Bu)$_2$] ligand, resulting in the diiron complex **1**. We posit that the amide groups are coordinated to the iron centers in the precursor, as shown on the right.

The ligand H[BPMP(NHCO^{t}Bu)$_2$] is first deprotonated by one equivalent of KOMe in methanol, then metallated with two equivalents of iron(II) triflate, Fe(OTf)$_2$·2CH$_3$CN, and finally, one equivalent of NaOAc·3H$_2$O is added for acetate to act as an additional bridge between the iron centers (see Scheme 1). The product is then worked up using the procedure mentioned in the SI and recrystallized to yield the precursor complex [Fe$_2$(BPMP(NHCOtBu)$_2$)(OAc)](OTf)$_2$ (**1**). Further characterization of this complex by UV-Vis spectroscopy shows a band at 389 nm, which shifts to 442 nm upon nitrosylation (see Figure S10). The 4.2-K/53-mT Mössbauer spectrum of this complex shows a single quadrupole doublet with an isomer shift (δ) of 1.19 mm/s and a quadrupole splitting parameter (ΔE_Q) of 2.85 mm/s, indicative of the presence of hs-Fe^{II} centers in this compound (see Figure 1).

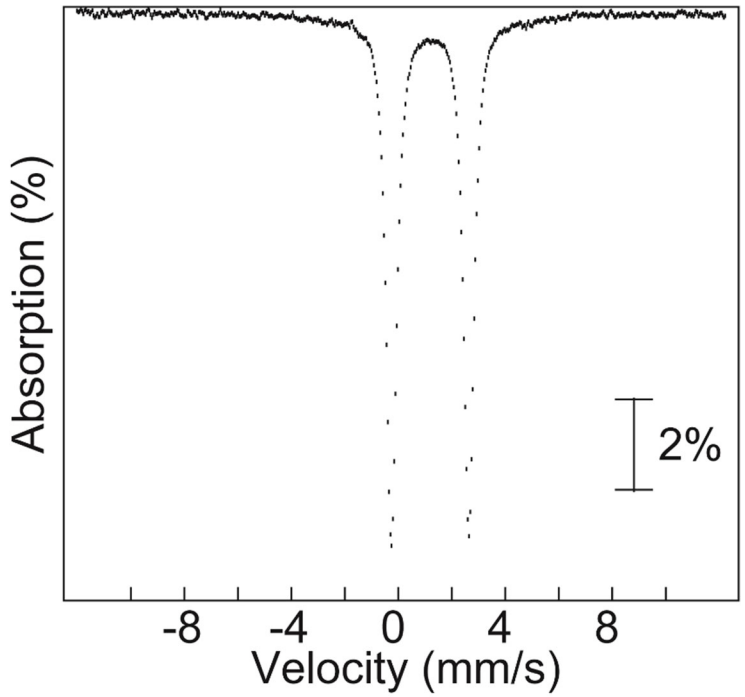

Figure 1. The Mössbauer spectrum of complex **1** shows a quadrupole doublet with δ = 1.19 mm/s and ΔE_Q = 2.85 mm/s, collected at 4.2 K and an applied magnetic field of 53 mT oriented parallel to the direction of propagation of the γ beam.

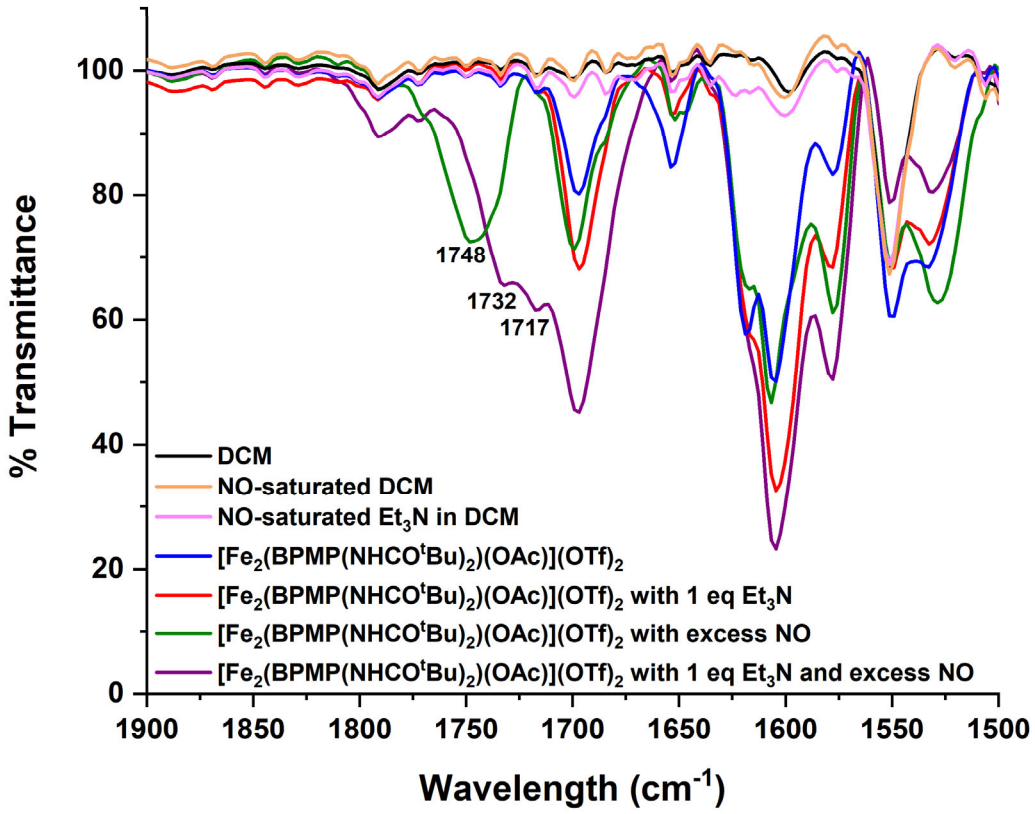

Figure 2. Overlay of the IR spectra of complex **1** and the corresponding reaction product with NO (**1/NO**) in dichloromethane (DCM), showing the formation of a new band at 1748 cm^{-1}, characteristic of the N-O stretch of hs-{FeNO}^{7} complexes (green line). In the presence of triethylamine as a base, the N-O stretching band shifts to lower energy (dark purple line) with distinct features at 1732 and 1717 cm^{-1}.

Reaction of complex **1** with an excess amount of NO gas in CH_2Cl_2 at 25 °C yielded a brown crystalline material after recrystallization (complex **1/NO**). IR spectroscopy shows a new signal at 1747 cm^{-1} for the resulting solid, indicating the formation of a hs-{FeNO}^{7} complex (see Figures S3 and S4). Reaction of complex **1** with NO in the presence of base produced a new hs-{FeNO}^{7} complex, evident from a shift of the N-O stretch from 1748 cm^{-1} (in solution) to lower energy, with two prominent features at 1732 and 1717 cm^{-1} (see Figure 2). A ^{15}NO experiment further supports the assignment of these peaks as N-O stretches (see Figure S9). This indicates that the amide groups can be deprotonated. Interestingly, X-ray crystallography of the product from the nitrosylation reaction of **1** in the presence of base revealed a new diiron mononitrosyl complex [Fe_2(BPMP(NHCO^{t}Bu)(NCO^{t}Bu))(OAc)(NO)](OTf) (**2**; see Figure 3).

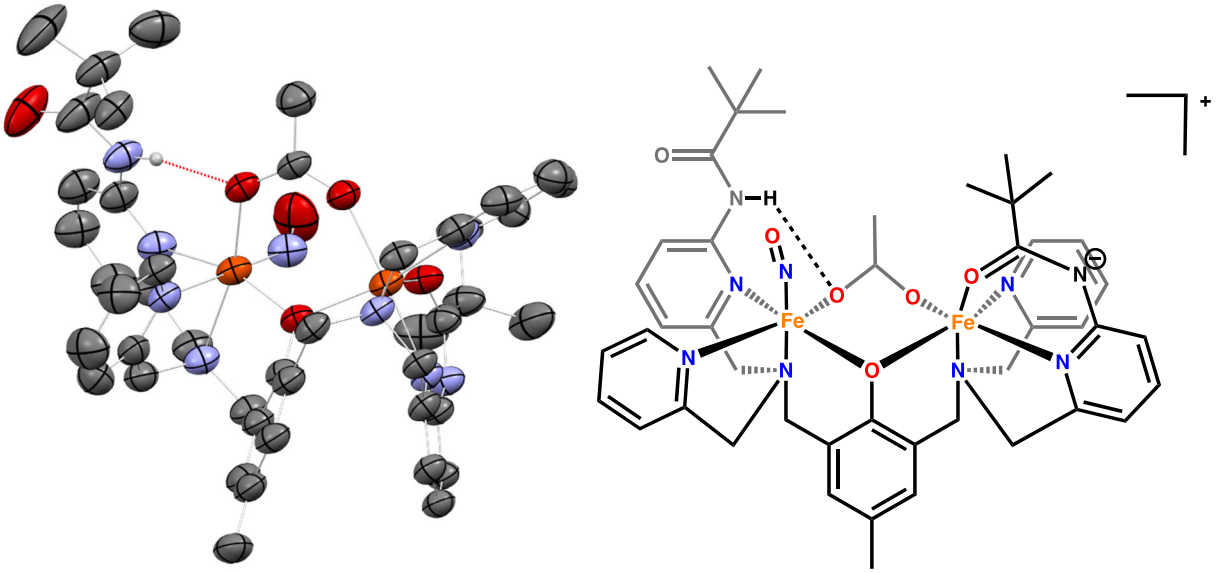

Figure 3. Crystal structure of complex **2** with ellipsoids drawn at 50% probability (CCDC# 2084747). The triflate counter anion, solvent molecules, and hydrogen atoms (except for N-H) are omitted for clarity.

EPR data of complex **1** in the presence of NO support the formation of a dinitrosyl species in solution after nitrosylation (EPR silent), which transforms into a mononitrosyl species upon the addition of base, evident from the appearance of an EPR signal around g = 2, typical for these species (see Figure S14).[23] These results strongly support the idea that upon deprotonation, the amide group coordinates strongly to one of the iron centers, stabilizing the diiron mononitrosyl core in **2**. In the EPR data, we frequently noticed a g = ~4.3 signal, indicating some kind of decomposition or oxidation of the complex. Characterization of this compound by X-ray crystallography yielded a surprising all-ferric triiron complex (**3**) as shown in Figure 4. EPR spectroscopy shows that this species indeed gives rise to the g = ~4.3 signal, as shown in Figure S15. Notably, in complex **3** the two oxo bridges are stabilized by hydrogen bonding to the amide groups in the SCS of the ligand, as indicated in Figure 4.

We further hypothesize that complex **1** binds NO only weakly in solution, due to the competitive ligation of the oxygen atoms of the amide groups, leading to a mixture of species, as indicated in Figure S7. The presence of multiple NO complexes in solution in these reactions is further suggested by the solution IR data in Figure 2, showing broad N-O stretching bands for both **1/NO** and **2**. The diiron mononitrosyl complex **2** was then recrystallized with NO-saturated DCM and NO-saturated hexanes.

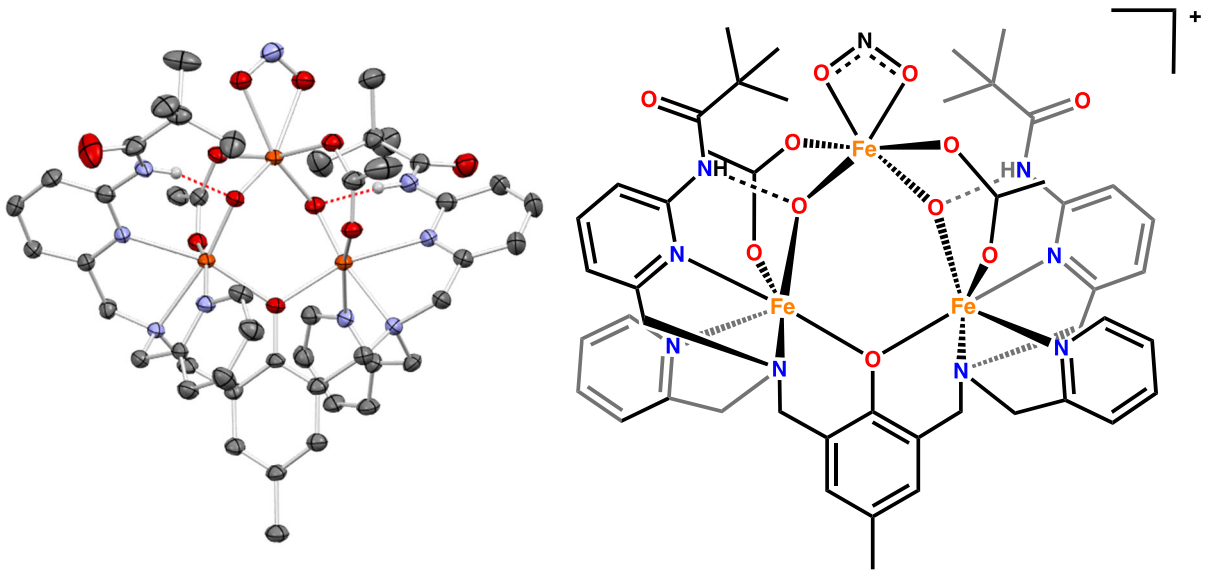

Figure 4. Crystal structure of the triiron complex [Fe_3(BPMP(NHCO^{t}Bu)$_2$(OAc)$_2$(μ-O)$_2$(ONO)](OTf) (**3**) with ellipsoids drawn at 50% probability (CCDC# 2126171). The triflate counter anion, solvent molecules, and hydrogen atoms (except for N-H) are omitted for clarity. The hydrogen bond (NH···O) distance is ~2.0 Å for both amides.

Complex **2** has a bent FeNO moiety typical for hs-{FeNO}^{7} complexes.[18, 23-27] It is important to note that the formation of diiron mononitrosyl complexes is rare in diiron systems. Complex **2** is only the second example of such a complex in the literature, the other example is the complex [Fe_2(*N*-Et-HPTB)(NO)(DMF)$_3$](BF$_4$)$_3$ reported by Majumdar and coworkers, which was generated by using a redox controlled strategy with a thioacetate-bridged precursor.[18, 23] The N–O and Fe–NO bond distances of complex **2** are 1.16(5) and 1.82(4) Å, respectively, which are very similar to those of the parent dinitrosyl complex, [Fe_2(BPMP)(OPr)(NO)$_2$](BPh$_4$)$_2$ (OPr$^-$ = propionate) (1.17 and 1.79 Å) without the amide groups in the SCS.[25] The Fe···Fe distance of complex **2** is 3.57 Å. Fe–O bond distances of the bridging phenolate are 2.02(3) and 2.10(3) Å, whereas those of the bridging acetate are 2.02(3) and 2.11(3) Å for the hs-{FeNO}^{7} moiety and the hs-Fe^{II} center, respectively. The Fe-O(amide) bond distance is 2.06(3) Å. The pendant amide forms a strong hydrogen bond with the bridging acetate ligand (NH···O distance: 2.10 Å; N···O distance: 2.95 Å). A similar hydrogen bond to the bridging carboxylate is also observed in the active site of *T. maritima* FDP, with residue Y197 proposed to be the hydrogen bond donor to the bridging carboxylate.[11]

In conclusion, we have synthesized a new model system for FNORs that can form a rare diiron mononitrosyl complex. The SCS amide groups in the ligand scaffold are versatile and can form a hydrogen bond to the bridging acetate ligand and/or affect the primary coordination sphere of the iron centers by coordinating to iron via their carbonyl oxygens. Deprotonation enhances binding to iron, blocking NO coordination, which allowed us to isolate a pure diiron mononitrosyl complex. Future studies will focus on exploring the potentially interesting electronic structure of **2**, and on designing a model system that allows for hydrogen bonding of the SCS groups to the NO ligand, without competing with NO for binding to the iron centers.

Corresponding Author
lehnertn@umich.edu

ORCID:
Nicolai Lehnert: 0000-0002-5221-5498
Hai T. Dong: 0000-0002-8914-3045
Abigail J. Bracken: 0000-0003-0988-1118
Michael O. Lengel: 0000-0002-1003-4357
Debangsu Sil: 0000-0002-0718-3925
Carsten Krebs: 0000-0002-3302-7053

Declaration of Competing Interest: The authors declare that they have no known competing financial interests or personal relationships that could have appeared to influence the work reported in this paper.

Acknowledgments: This work was supported by the National Science Foundation (CHE-2002885 to NL) and by the National Institutes of Health (GM-127079 to CK). We thank Dr. Jeff Kampf (University of Michigan) for X-ray crystallographic analysis of complexes **2** and **3**, and acknowledge funding from NSF grant CHE-0840456 for X-ray instrumentation. YZ acknowledges Fudan University for a summer research fellowship that allowed her to come to the University of Michigan. AJB acknowledges the 2021 LSA Summer Research Fellowship from the University of Michigan.

TOC Figure:

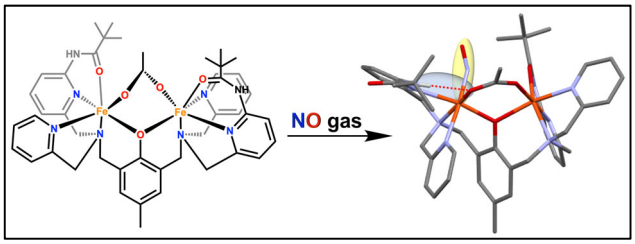

Reference:

1. Lehnert, N.; Berto, T. C.; Galinato, M. G. I.; Goodrich, L. E., The Role of Heme-Nitrosyls in the Biosynthesis, Transport, Sensing, and Detoxification of Nitric Oxide (NO) in Biological Systems: Enzymes and Model Complexes. In *The Role of Heme-Nitrosyls in the Biosynthesis, Transport, Sensing, and Detoxification of Nitric Oxide (NO) in Biological Systems: Enzymes and Model Complexes*, Kadish, K. M.; Smith, K. M.; Guilard, R., Eds. World Scientific: New Jersey, 2011; Vol. 14,, pp 1-247
2. Ignarro, L., *Nitric Oxide: Biology and Pathobiology*. Academic Press: San Diego, 2000.
3. Wink, D. A.; Mitchell, J. B., Chemical biology of nitric oxide: insights into regulatory, cytotoxic, and cytoprotective mechanisms of nitric oxide. *Free Rad. Biol. Med.* **1998,** *25*, 434-456.
4. Lehnert, N.; Kim, E.; Dong, H. T.; Harland, J. B.; Hunt, A. P.; Manickas, E. C.; Oakley, K. M.; Pham, J.; Reed, G. C.; Alfaro, V. S., The Biologically Relevant Coordination Chemistry of Iron and Nitric Oxide: Electronic Structure and Reactivity. *Chem. Rev.* **2021**, *121*, 14682-14905.
5. Stuehr, D. J.; Gross, S. S.; Sakuma, I.; Levi, R.; Nathan, C. F., Activated Murine Macrophages Secrete a Metabolite of Arginine with the Bioactivity of Endothelium-Derived Relaxing Factor and the Chemical Reactivity of Nitric Oxide. *J. Exp. Med.* **1989,** *169*, 1011-1020.
6. MacMicking, J.; Xie, Q.-W.; Nathan, C., Nitric Oxide and Macrophage Function. *Annu. Rev. Immunol.* **1997,** *15*, 323-350.
7. Gardner, A. M.; Gessner, C. R.; Gardner, P. R., Regulation of the Nitric Oxide Reduction Operon (*norRVW*) in *Escherichia coli*. Role of NorR and σ^{54} in the Nitric Oxide Stress Response. *J. Biol. Chem.* **2003,** *278*, 10081-10086.
8. Missall, T. A.; Lodge, J. K.; McEwen, J. E., Mechanisms of Resistance to Oxidative and Nitrosative Stress: Implications for Fungal Survival in Mammalian Hosts. *Eucaryot. Cell* **2004,** *3*, 835-846.
9. Sarti, P.; Fiori, P. L.; Forte, E.; Rappelli, P.; Teixeira, M.; Mastronicola, D.; Sanciu, G.; Giuffré, A.; Brunori, M., *Trichomonas vaginalis* degrades nitric oxide and expresses a flavorubredoxin-like protein: a new pathogenic mechanism? *Cell. Mol. Life Sci.* **2004,** *61*, 618-623.
10. Frazão, C.; Silva, G.; Gomes, C. M.; Matias, P.; Coelho, R.; Sieker, L.; Macedo, S.; Liu, M. Y.; Oliveira, S.; Teixeira, M.; Xavier, A. V.; Rodrigues-Pousada, C.; Carrondo, M. A.; Le Gall, J., Structure of a dioxygen reduction enzyme from *Desulfovibrio gigas*. *Nat. Struct. Biol.* **2000,** *7*, 1041-1045.
11. Silaghi-Dumitrescu, R.; Kurtz, D. M., Jr.; Ljungdahl, L. G.; Lanzilotta, W. N., X-ray Crystal Structures of *Moorella thermoacetica* FprA. Novel Diiron Site Structure and Mechanistic Insights into a Scavenging Nitric Oxide Reductase. *Biochemistry* **2005,** *44*, 6492-6501.
12. Mills, P. C.; Rowley, G.; Spiro, S.; Hinton, J. C. D.; Richardson, D. J., A combination of cytochrome c nitrite reductase (NrfA) and flavorubredoxin (NorV) protects Salmonella enterica serovar Typhimurium against killing by NO in anoxic environments. *Microbiology* **2008,** *154* (4), 1218-1228.
13. Gomes, C. M.; Giuffrè, A.; Forte, E.; Vicente, J. B.; Saraiva, L. M.; Brunori, M.; Teixeira, M., A Novel Type of Nitric-oxide Reductase. *Escherichia Coli* Flavorubredoxin. *J. Biol. Chem.* **2002,** *277*, 25273-25276.
14. Lehnert, N.; Fujisawa, K.; Camarena, S.; Dong, H. T.; White, C. J., Activation of Non-Heme Iron-Nitrosyl Complexes: Turning up the Heat. *ACS Catal.* **2019,** *9*, 10499-10518.

15. Pal, N.; Jana, M.; Majumdar, A., Reduction of NO by diiron complexes in relation to flavodiiron nitric oxide reductases. *Chem. Commun.* **2021,** *57*, 8682-8698.
16. Enemark, J. H.; Feltham, R. D., Principles of Structure, Bonding, and Reactivity for Metal Nitrosyl Complexes. *Coord. Chem. Rev.* **1974,** *13*, 339-406.
17. Dong, H. T.; White, C. J.; Zhang, B.; Krebs, C.; Lehnert, N., Non-Heme Diiron Model Complexes Can Mediate Direct NO Reduction: Mechanistic Insight into Flavodiiron NO Reductases. *J. Am. Chem. Soc.* **2018,** *140*, 13429-13440.
18. Jana, M.; White, C. J.; Pal, N.; Demeshko, S.; Meyer, F.; Lehnert, N.; Majumdar, A., Functional Models for the Mono- and Dinitrosyl Intermediates of FNORs: Semireduction versus Superreduction of NO. *J. Am. Chem. Soc.* **2020,** *142*, 6600-6616.
19. White, C. J.; Speelman, A. L.; Kupper, C.; Demeshko, S.; Meyer, F.; Shanahan, J. P.; Alp, E. E.; Hu, M.; Zhao, J.; Lehnert, N., The Semireduced Mechanism for Nitric Oxide Reduction by Non-Heme Diiron Complexes: Modeling Flavodiiron Nitric Oxide Reductases. *J. Am. Chem. Soc.* **2018,** *140*, 2562-2574.
20. Jiang, Y.; Hayashi, T.; Matsumura, H.; Do, L. H.; Majumdar, A.; Lippard, S. J.; Moënne-Loccoz, P., Light-Induced N_2O Production from a Non-heme Iron–Nitrosyl Dimer. *J. Am. Chem. Soc.* **2014,** *136*, 12524-12527.
21. Khatua, S.; Majumdar, A., Flavodiiron Nitric Oxide Reductases: Recent Developments in the Mechanistic Study and Model Chemistry for the Catalytic Reduction of NO. *J. Inorg. Biochem.* **2015,** *142*, 145-153.
22. Comba, P.; Gahan, L. R.; Mereacre, V.; Hanson, G. R.; Powell, A. K.; Schenk, G.; Zajaczkowski-Fischer, M., Spectroscopic Characterization of the Active $Fe^{III}Fe^{III}$ and $Fe^{III}Fe^{II}$ Forms of a Purple Acid Phosphatase Model System. *Inorg. Chem.* **2012,** *51*, 12195-12209.
23. Jana, M.; Pal, N.; White, C. J.; Kupper, C.; Meyer, F.; Lehnert, N.; Majumdar, A., Functional Mononitrosyl Diiron(II) Complex Mediates the Reduction of NO to N_2O with Relevance for Flavodiiron NO Reductases. *J. Am. Chem. Soc.* **2017,** *140*, 14380-14383.
24. Berto, T. C.; Hoffman, M. B.; Murata, Y.; Landenberger, K. B.; Alp, E. E.; Zhao, J.; Lehnert, N., Structural and Electronic Characterization of Non-Heme Fe(II)-Nitrosyls as Biomimetic Models of the Fe_B Center of Bacterial Nitric Oxide Reductase (NorBC). *J. Am. Chem. Soc.* **2011,** *133*, 16714–16717.
25. Zheng, S.; Berto, T. C.; Dahl, E. W.; Hoffman, M. B.; Speelman, A. L.; Lehnert, N., The Functional Model Complex $[Fe_2(BPMP)(OPr)(NO)_2](BPh_4)_2$ Provides Insight into the Mechanism of Flavodiiron NO Reductases. *J. Am. Chem. Soc.* **2013,** *135*, 4902−4905.
26. Dong, H. T.; Speelman, A. L.; Kozemchak, C. E.; Sil, D.; Krebs, C.; Lehnert, N., The $Fe_2(NO)_2$ Diamond Core: A Unique Structural Motif in Non-Heme Iron-NO Chemistry. *Angew. Chem. Int. Ed.* **2019,** *131* (49), 17859-17863.
27. Berto, T. C.; Speelman, A.; Zheng, S.; Lehnert, N., Mono- and Dinuclear Non-Heme Iron-Nitrosyl Complexes: Models for Key Intermediates in Bacterial Nitric Oxide Reductases. *Coord. Chem. Rev.* **2013,** *257*, 244-259.